Emission Mössbauer Spectroscopy study of fluence dependence of paramagnetic relaxation in Mn/Fe implanted ZnO

H. Masenda[a*], S. Geburt[b], K. Bharuth-Ram[c], D. Naidoo[a], H. P. Gunnlaugsson[d], K. Johnston[d], R. Mantovan[e], T. E. Mølholt[d], M. Ncube[a], S. Shayestehaminzadeh[f] H. P. Gislason[g], G. Langouche[h], S. Ólafsson[g], C. Ronning[b] and ISOLDE Collaboration

[a]*School of Physics, University of the Witwatersrand, Johannesburg, 2050, South Africa,*

[b]*Institue of Solid State Physics, University of Jena, 07743, Jena, Germany*

[c]*Physics Department, Durban University of Technology, Durban 4001, South Africa,*

[d]*PH Dept, ISOLDE/CERN, 1211 Geneva 23, Switzerland,*

[e]*Laboratorio MDM, IMM-CNR, Via Olivetti 2, 20864 Agrate Brianza (MB), Italy,*

[f]*Institute of Materials Chemistry, RWTH Aachen University, Kopernikusstr. 10, 52074 Aachen, Germany*

[g]*Science Institute, University of Iceland, Dunhaga 3,107 Reykjavík, Iceland,*

[h]*KULeuven, Instituut voor Kern-en Stralingsfysica, 3001 Leuven, Belgium,*

Abstract

Emission Mössbauer Spectroscopy following the implantation of radioactive precursor isotope $^{57}Mn^{*}$ ($t_{½}$ = 1.5 min) at ISOLDE/CERN show that a large fraction of ^{57}Fe atoms produced in the ^{57}Mn beta decay are trapped as paramagnetic Fe^{3+} with relatively long spin-lattice relaxation times in ZnO. We have extended this study to eMS studies on ZnO pre-implanted with ^{56}Fe to fluences of 2×10^{13}, 5×10^{13} and 8×10^{13} ions/cm^2, in order to investigate the dependence of the paramagnetic relaxation rate with fluence. The spectra in the present samples are also dominated by magnetic features displaying paramagnetic relaxation effects. The extracted spin-lattice relaxation rates show a slight increase with increasing ion fluence at corresponding temperatures and the area fraction of Fe^{3+} at room temperature reach a maximum contribution in studied fluence range.

Keywords: ZnO, Fe implantation, emission Mössbauer spectroscopy, spin-lattice relaxation

*Contact author: hilary.masenda@wits.ac.za

Introduction

In the midst of many reports with mixed conclusions on the nature of magnetism in Fe doped ZnO [1, 2, 3, 4, 5, 6, 7], we have reported results of emission Mössbauer spectroscopy (eMS) on virgin ZnO single crystals following $^{57}Mn^{+}$ implantation with a fluence of ~3×10^{12} ions/cm^2 [8, 9] and over a wide range of ion fluence [10]. The absence of ordered magnetism (above 90 K) in extremely dilute doped ZnO was unequivocally proven through angle dependent eMS measurements in the presence of an external magnetic field of 0.6 T [8]. The emission Mössbauer spectra exhibited paramagnetism, resulting from Fe^{3+} located on Zn substitutional sites weakly coupled to the lattice and showing temperature dependent spin-lattice relaxation. The Fe^{3+} spin-lattice relaxation rate was found to follow an unusual T^9 temperature dependence [9].

Moreover, we have conducted eMS and X-ray Magnetic Circular Dichroism (XMCD) studies [10] on the effect of fluence (increase in 3*d*-atoms concentration) on the magnetic contribution in ZnO samples implanted with Fe with atomic concentrations in two regimes, 0.1 – 6.4×10^{-4} at.% and 0.02 – 2.2 at.%. In the latter concentration range, a transition to spin-spin relaxation effects between neighbouring Fe^{3+} ions was observed from the spin-lattice relaxation observed at the lower concentration regime. In this paper, we focus on the magnetic contribution and on spin-lattice relaxation in ZnO crystals implanted with Fe with atomic concentrations in the range 0.49×10^{-2} – 1.97×10^{-2} at.%, which cover the upper intermediate region of atomic concentration not reported in similar previous studies [10].

Experimental Details

Commercially acquired ZnO single crystals (Crystec GmbH) were implanted with ^{56}Fe ions using a multipurpose ion implanter, with implantation energy of 60 keV and at an angle of 7° to avoid channelling effects. Three ZnO samples were pre-implanted with ^{56}Fe ions to fluences of 2×10^{13}, 5×10^{13} and 8×10^{13} ions/cm^2. The corresponding atomic concentrations integrated over the ^{57}Mn profile are 0.49×10^{-2}, 1.23×10^{-2} and 1.97×10^{-2} at.%, respectively.

^{57}Fe eMS measurements were conducted utilising implantation of radioactive $^{57}Mn^{+}$ ions ($T_{1/2}$ = 1.5 min) at the ISOLDE facility at CERN. The beam is produced by 1.4 GeV proton- induced fission in an UC_2 target and multi-stage subsequent laser ionization. Pure beams with intensities ≤ 5×10^{8} ions/s and 40 keV energy were implanted at 30° relative to the sample normal into the ZnO single crystals held at temperatures ranging from room temperature to 570 K. eMS spectra were measured using a parallel plate avalanche detector equipped with a ^{57}Fe enriched stainless

steel electrode, mounted on a conventional drive system outside the implantation chamber at 60° relative to the sample normal. Isomer shifts and velocities are given relative to the centre of the spectrum of α-Fe at room temperature.

Analysis and results

The emission Mössbauer spectra obtained for the 8×10^{13} (ZnO:^{56}Fe8) and 5×10^{13} ions/cm^2 (ZnO:^{56}Fe5) pre-implanted ZnO samples, together with the fitted spectral components, are shown in Figure 1.

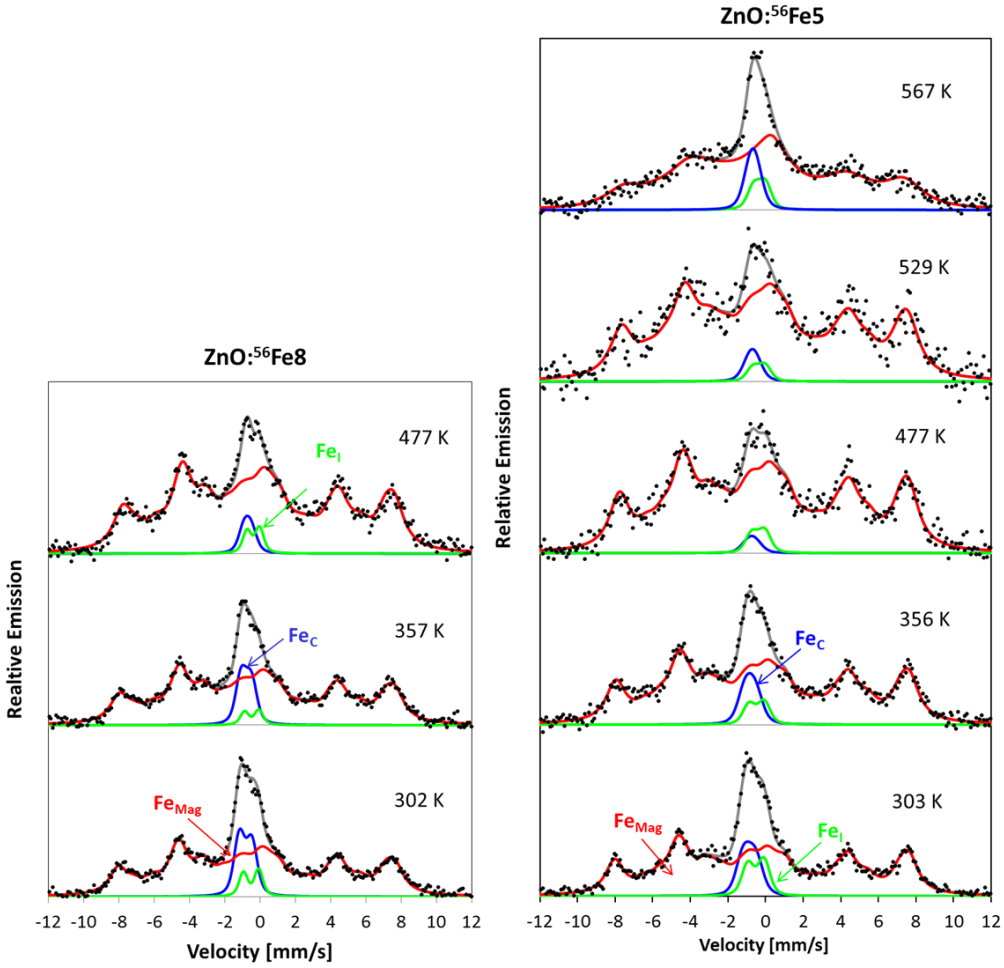

Figure 1: **Emission Mössbauer spectra (eMS) of ZnO pre-implanted with ^{56}Fe at ion fluences (left) 8×10^{13} and (right) 5×10^{13} ions/cm^2 as a function of temperature.**

The spectra were analysed using the Vinda program [11]. The analysis procedure and assignment of spectral components adopted here is similar to that applied in our earlier studies on virgin ZnO [8, 9]. The observed magnetic structure assigned to high-spin Fe^{3+} (labelled Fe_{Mag}) was analysed using the empirical model based on the Blume-Tjon (BT) [12] line-shape as described by Mølholt *et al.* [9, 13]. In the final fitting procedure, the magnetic feature was fitted

with five BT sextets. This empirical model cannot determine the exact isomer shift or quadrupole splitting, but can determine the spin relaxation rates of Fe^{3+} and the maximum magnetic hyperfine splitting. The central regions of the spectra were fitted with two doublets attributed to Fe in the 2+ state on regular crystalline sites (Fe_C) and Fe on interstitial sites (Fe_I) as described by Gunnlaugsson *et al.* [8]. The hyperfine parameters extracted at room temperature for all three samples are presented in Table 1.

Table 1: Room temperature hyperfine parameters extracted for ZnO pre-implanted with ^{56}Fe at indicated ion fluences.

	ZnO:^{56}Fe2 (2×10^{13} ions/cm^2)		**ZnO:^{56}Fe5 (5×10^{13} ions/cm^2)**		**ZnO:^{56}Fe8 (8×10^{13} ions/cm^2)**	
Components	**Fe_C**	**Fe_I**	**Fe_C**	**Fe_I**	**Fe_C**	**Fe_I**
δ (mm/s)	0.93(2)	0.47(2)	0.84(1)	0.51(2)	0.82(2)	0.51(1)
ΔE_Q (mm/s)	-0.44(3)	0.85(2)	-0.66(3)	0.85(1)	-0.70(3)	0.86(1)

The temperature dependence of the quadrupole splitting, $\Delta E_Q(T)$ for Fe_C was restricted to follow Ingalls [14] prediction as was followed in Gunnlaugsson *et al.* [15] and is given by the expression,

$$\Delta E_Q(T) = \Delta E_{Q,Lat} + \Delta E_{Q,Val} \tanh\left(\frac{E_0}{2k_B T}\right) \quad (1)$$

where $\Delta E_{Q,Lat}$ is the contribution from non-cubic arrangement of lattice atoms, $\Delta E_{Q,Val}$ is the valence contribution resulting from Fe in z^2 *d* orbitals, E_0 is the splitting energy between the z^2 and x^2-y^2 orbitals. A quadrupole splitting value of -0.70(3) mm/s was obtained for Fe_C and a crystal field splitting value of E_0 =18(1) meV was determined for the high fluence implanted sample (ZnO:^{56}Fe8) using $\Delta E_{Q,Lat}$ and $\Delta E_{Q,Val}$ values of +0.12 mm/s and -2.5 mm/s, respectively, as reported by Gunnlaugsson *et al.* [15].

For the ZnO:^{56}Fe5 sample, a quadrupole splitting value of -0.66(3) mm/s was determined for Fe_C which is slightly smaller in magnitude compared with the value of -0.70(3) mm/s obtained for the ZnO:^{56}Fe8 sample. The E_0 value for this sample was determined to be 17(1) meV.

The ZnO:^{56}Fe2 sample was characterised with a ΔE_Q value of -0.44(2) mm/s for Fe_C which is equivalent to the value of -0.44(3) mm/s reported for virgin ZnO [8]. The resulting E_0 value of 12(3) meV is comparable to the value of 10 meV reported for virgin ZnO [9] considering the relative large error.

Discussion

The increase in the magnitude of the quadrupole splitting with increasing fluence suggests a loss of symmetry at the nucleus of the Fe atoms, resulting from an increase in lattice distortions with increasing implantation fluence. On the other hand, the decrease in the isomer shift values of Fe_C with increasing implantation fluence reflects an increase in the *s*-electron density at the nucleus of the probe atoms which attests to the strengthening of the bonds between the substitutional Fe atoms and the surrounding lattice atoms. For the samples under study, the hyperfine parameters for the interstitial component (Fe_I) are in agreement with values of δ = 0.50 mm/s and ΔE_Q = 0.85 mm/s, reported in ref [8].

The relaxation rates are related to the temperature dependent line broadening ($\Delta\Gamma$) of the sextets as described by Mølholt *et al*. [13]. Generally, it is expected that the spin lattice relaxation rate increases with increasing temperature because of the temperature dependence of the population of the phonon states [16]. The relaxation rates obtained from this study are shown in Figure 2 and are compared with those reported for virgin single crystal ZnO and α-Al_2O_3 reported in ref [9].

A deviation from a ~T^9 temperature dependence of the relaxation rates in virgin is observed. The data is consistent with additional spin-spin relaxation rates to the temperature dependent sin-lattice relaxation rates. These spin-spin interaction become dominant above when the concentration Fe ions is above 0.2 at.% [10]. Thus, the three measured concentrations lie just below this threshold.

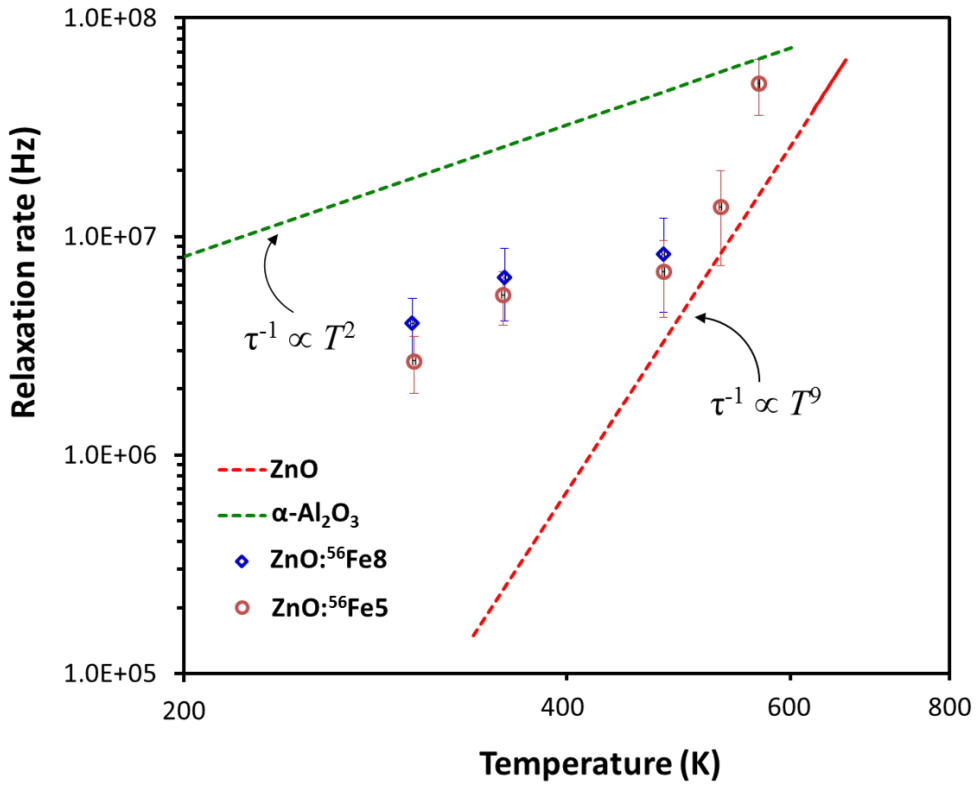

Figure 2: **Temperature dependent relaxation rates of the pre-implanted ZnO samples as a function of indicated fluence compared with trends in virgin ZnO and α-Al_2O_3. [Adapted from Mølholt *et al.* [9]]**

The relaxation rates of the ZnO:^{56}Fe5 and ^{56}Fe8 pre-implanted samples shows slight tendency to increase with increasing fluence at equivalent temperatures. This may be attributed to the increase in spin density by the increasing Fe fluence, with a consequential increase in spin-lattice relaxation rate. For the ZnO:^{56}Fe8 sample, the three temperatures show a trend which approximates a T^2 temperature-dependent relaxation rate which agrees with the measurements at equivalent temperatures for ZnO:^{56}Fe5. For ZnO:^{56}Fe5 there is deviation from this behaviour at highest temperature. This seems to suggest two different relaxation processes taking place in the measured temperature range for the ZnO:^{56}Fe5 sample. The spectra for the 2×10^{13} ions/cm^2 (ZnO:^{56}Fe2) pre-implanted sample were unfortunately associated with additional broadening due to vibrations in the experimental set-up and hence could not be used to extract the relaxation rates but was sufficient to give the area fraction of the Fe^{3+} at room temperature.

The area fractions extracted at room temperature for Fe^{3+} as a function of concentration, together with results obtained from earlier studies reported by Mantovan *et al.* [10], are presented in Figure 3. This investigation showed at low concentrations up to about ~1.7×10^{-4} at.%, the fraction of Fe^{3+} steadily increases at the expense of Fe^{2+} reaching at maximum of

approximately 80(3) %. For the three samples studied here, no significant changes in spectral features are observed at RT and the area fraction of the magnetic component (Fe_{Mag}) constitutes ~80(3) % of the spectral area. Figure 3 shows that Fe_{Mag} reaches a flattened maximum at the fluences used in the present work suggesting that Fe^{3+} is stabilised in samples with concentrations in the range of 0.49×10^{-2} – 1.97×10^{-2} at.%. On the other hand, at concentrations above 0.02 at.%, Fe^{2+} in the form of Fe_C and Fe_D (implantation-induced damage) dominates suggesting that Fe-related donors dominate and in turn favour the formation of Fe^{2+} state over Fe^{3+} [10].

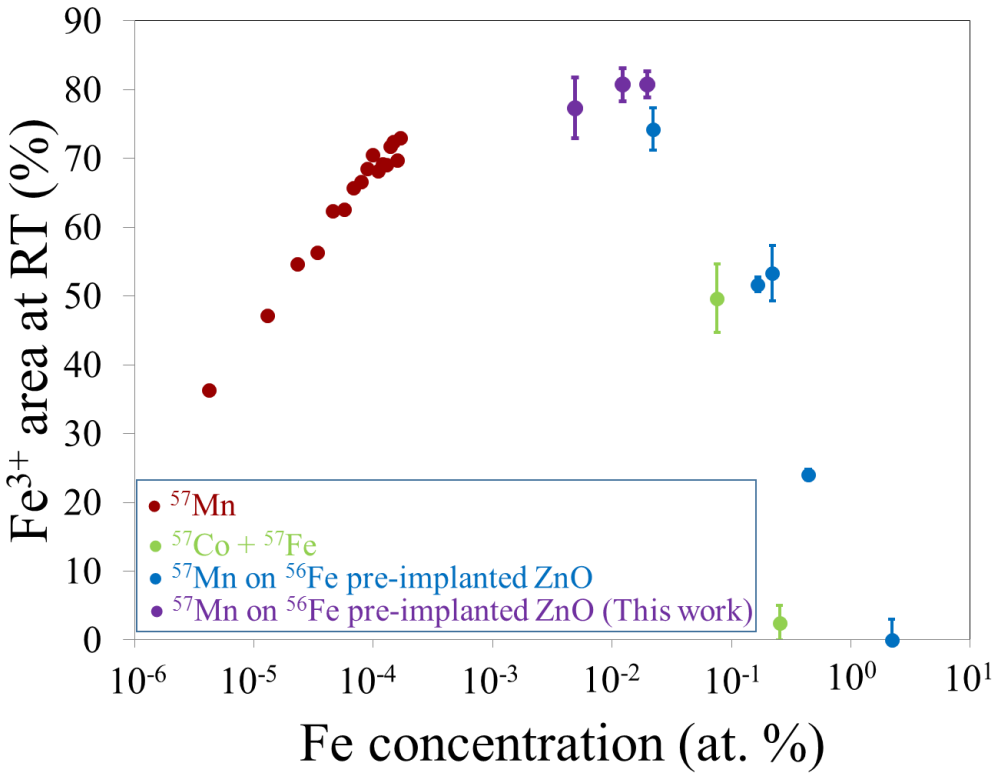

Figure 3: **Concentration dependence of the area fraction of Fe^{3+} at room temperature. Results of the present measurements are included in the data adopted from ref. [10].**

The results in Figure 3 indicate that the contribution of Fe^{3+} reaches a saturation for concentration in the range of 5×10^{-3} to 5×10^{-1} at.% (10^{12} – 10^{14} ions/cm^2). For concentrations below ~5×10^{-3} at.%, the Fe^{3+} state is unstable and the area fraction of the Fe^{3+} can be 'reset' by annealing of the ZnO sample, as reported by Naidoo *et al.* [17], while above a fluence of 10^{14} ions/cm^2, only Fe^{2+} dominates the eMS spectra.

Conclusions

eMS measurements were conducted on three ZnO single crystal samples pre-implanted with ^{56}Fe to fluences of 2×10^{13} , 5×10^{13} and 8×10^{13} ions/cm^2. The spectra are dominated by magnetic features attributed to paramagnetic Fe^{3+} in defect complexes which show relatively long spin-lattice relaxation times. Spin relaxation rates extracted from the analysis shows a relatively small increasing tendency with implanted fluence at corresponding temperatures. The area fraction of the paramagnetic Fe^{3+} shows a maximum contribution of approximately 80(3) % of the spectra at room temperature for the three fluences.

Acknowledgements

This work was supported by the European Union Seventh Framework through ENSAR (contract no. 262010) and the German BMBF under Contract No. 05KK4TS1/9. H. Masenda, K. Bharuth-Ram, D. Naidoo and M. Ncube acknowledge support from the South African National Research Foundation and the Department of Science and Technology within the SA-CERN programme. T. E. Mølholt, S. Shayestehaminzadeh, H. P. Gíslason and S. Ólafsson support from the Icelandic Research Fund. We acknowledge support from the Deutsche Forschungsgemeinschaft (Ro1198/13-1). R. Mantovan acknowledges support from MIUR through the FIRB Project RBAP115AYN "Oxides at the nanoscale: multifunctionality and applications".

References

[1] C. Liu, F. Yun and H. Morkoç, *J. Mater. Sci. Mater. Electron.,* vol. 16, p. 555, 2005.

[2] Ü. Özgür, Y. I. Alivov, C. Liu, A. Teke, M. A. Reshchikov, S. Doğan, V. Avrutin, S.-J. Cho and H. Morkoç, *J. Appl. Phys.,* vol. 98, p. 041301, 2005.

[3] K. Ando, *Science,* vol. 312, p. 1883, 2006.

[4] V. Avrutin, N. Izyumskay, U. Ozgur, D. J. Silversmith and H. Morkoc, *Proc. IEEE,* vol. 98, p. 1288, 2010.

[5] T. Dietl, *Nature. Mater.,* vol. 9, p. 965, 2010.

[6] A. Zunger, S. Lany and H. Raebiger, *Physics,* vol. 3, p. 53, 2010.

[7] L. Pereira, J. Araujo, U. Wahl, S. Decoster, M. Van Bael, K. Temst and A. Vantomme, *J. Appl. Phys.,* vol. 113, p. 023903, 2013.

[8] H. P. Gunnlaugsson, T. E. Mølholt, R. Mantovan, H. Masenda, D. Naidoo, W. B. Dlamini, R. Sielemann, K. Bharuth-Ram, G. Weyer, K. Johnston, G. Langouche, S. Ólafsson, H. P. Gíslason, Y. Kobayashi, Y. Yoshida, M. Fanciulli and the ISOLDE Collaboration, *Appl. Phys. Lett.*, vol. 97, p. 142501, 2010.

[9] T. E. Mølholt, H. P. Gunnlaugsson, K. Johnston, R. Mantovan, H. Masenda, D. Naidoo, S. Ólafsson, K. Bharuth-Ram, H. P. Gislason, G. Langouche, R. Sielemann, G. Weyer and t. I. Collaboration, *Phys. Scr.*, vol. T148, p. 014006, 2012.

[10] R. Mantovan, H. P. Gunnlaugsson, K. Johnston, H. Masenda, T. E. Mølholt, D. Naidoo, M. Ncube, S. Shayestehaminzadeh, K. Bharuth-Ram, M. Fanciulli, H. P. Gíslason, G. Langouche, S. Ólafsson, L. M. C. Pereira, U. Wahl, P. Torelli and G. Weyer, *Adv. Electron. Mater.*, vol. 1, p. 1400039, 2015.

[11] H. P. Gunnlaugsson, *Hyp. Int.*, 2015 (Accepted).

[12] M. Blume and J. A. Tjon, *Phys. Rev.*, vol. 165, p. 446, 1968.

[13] T. E. Mølholt, R. Mantovan, H. P. Gunnlaugsson, D. Naidoo, S. Ólafsson, K. Bharuth-Ram, M. Fanciulli, K. Johnston, Y. Kobayashi, G. Langouche, H. Masenda, R. Sielemann, G. Weyer and H. P. Gíslason, *Hyp. Int.* , vol. 197, p. 89, 2010.

[14] R. Ingalls, *Phys. Rev.*, vol. 133, p. A787, 1964.

[15] H. P. Gunnlaugsson, K. Johnston, T. E. Mølholt, G. Weyer, R. Mantovan, H. Masenda, D. Naidoo, S. Ólafsson, K. Bharuth-Ram, H. P. Gíslason, G. Langouche, M. B. Masden and t. I. Collab, *Appl. Phys. Lett.*, vol. 100, p. 042109, 2012.

[16] S. Mørup, in *Mössbauer Spectroscopy and Transition Metal Chemistry: Fundamentals and Application*, P. Gütlich, E. Bill and A. X. Trautwein, Eds., Berlin, Springer, 2010.

[17] P. Raj and S. K. Kulshreshtha, *Phys. Stat. Sol. (A)*, vol. 4, p. 501, 1971.

[18] D. Naidoo, H. P. Gunnlaugsson, T. E. Mølholt, R. Mantovan, H. Masenda, K. Bharuth-Ram, K. Johnston, H. P. Gislason, G. Langouche and S. Ólafsson, *Hyp. Int.*, vol. 221, p. 45, 2013.